Investigation of the $Al^{27}(\alpha,p)$ Reaction by Cross-Section Fluctuation Studies*

G. DEARNALEY
Atomic Energy Research Establishment, Harwell, England†

AND

W. R. GIBBS, R. B. LEACHMAN, AND P. C. ROGERS‡
University of California, Los Alamos Scientific Laboratory, Los Alamos, New Mexico

(Received 26 April 1965)

Cross sections for the reaction $Al^{27}(\alpha,p)Si^{30}$ have been measured with energy resolutions which, in the incoming alpha-particle channel, are finer than the energy width of the overlapping levels of the compound system P^{31}. Fluctuations in these cross sections were analyzed for the coherence widths of this compound nucleus and for details of the reaction mechanism, such as the behavior of reaction amplitudes as shown by the form of the frequency distribution of the cross section, the independence of the reactions leading to the different magnetic substates, and the amounts of compound-nucleus and direct-interaction processes. Cross sections were measured at 11 angles between 0° and 175° and at 5-keV energy steps for energies between 5.8 and 8.6 MeV. Lack of a cross correlation between the yields of protons to the ground (0^+) and first excited (2^+) states of Si^{30} confirmed the expected overlapping of levels of the compound nucleus, which is a basic requirement of fluctuation analysis. The coherence width of the compound-nucleus P^{31} was found to increase from 8 to 18 keV over the range of excitation energy 14.7 to 17.1 MeV. At the back angles of 175° and 170° the frequency distributions of cross sections for protons to the ground state of Si^{30} agree with χ^2 distributions with only slightly more than two effective degrees of freedom. This number corresponds to the slightly more than one effective magnetic substate allowed by angular-momentum properties near 180°. This agreement substantiates cross-section fluctuation theory and indicates negligible direct interaction at these back angles. At 140° and 160° direct interactions were assumed still to be negligible, and then from the frequency distributions of cross sections the number of independent magnetic quantum states at these angles was found to be less than expected from an analysis based on angular-momentum properties and a Hauser-Feshbach calculation. This difference is a consequence of the small orbital angular momenta involved in the (α,p) reaction at these energies. These effective numbers of magnetic substates were used at the corresponding forward angles to determine the amounts of compound-nucleus and direct-interaction processes from fluctuations in cross sections. At the lowest energies of incident alpha particles the amount of direct interaction was too low to be determined with accuracy, but at the highest energies the maximum direct-interaction cross section was roughly equal to the compound-nucleus cross section. The direct-interaction cross section was found to vary with angle roughly as expected from distorted-wave Born-approximation calculations.

I. INTRODUCTION

MANY measurements of fluctuations in nuclear reaction cross sections have now been made at suitably high excitation energies. Use of the analyses introduced by Ericson[1,2] and by Brink and Stephen[3] has allowed studies of several nuclear properties that are not readily investigated by other means. One of the quantities most easily determined by this means is the average width of the levels, which is the coherence width Γ, even though the levels at these excitation energies are broadly overlapping. Another goal has been to test the currently accepted formalisms for nuclear reactions as they apply particularly to the slowest, compound-nucleus reactions. With these foundations established, fluctuation theory can be generally useful in distinguishing between slow and fast (direct-interaction) processes for a variety of possible reactions and at various angles of emission. In the present experiment, the $Al^{27}(\alpha,p)Si^{30}$ reaction has been extensively studied for these purposes.

Certain conditions must be met to obtain sensitivity in these analyses. One of the most important is that the number of incoherent waves contributing to the reaction should be minimized. As an example of the damping from incoherent waves, the fluctuations in the cross section σ integrated over all angles are reduced by the incoherent combination of the waves corresponding to the various orbital angular momenta[2]; thus, the conveniently measured $Si^{28}(n,\alpha)Mg^{25}$ cross section[4,5] particularly suffers in sensitivity for fluctuation studies. Even for differential cross sections $\sigma(\theta)$, for which the waves corresponding to different orbital angular momenta combine coherently, the amplitudes of different magnetic substates combine incoherently and damp the fluctuations. This again decreases the sensitivity of the analyses. For this reason, the differ-

* Work performed under the auspices of the U. S. Atomic Energy Commission.

† Work done at the Los Alamos Scientific Laboratory while on extended duty from the Atomic Energy Research Establishment.

‡ Present address: Brookhaven National Laboratory, Upton, New York.

[1] T. Ericson, Ann. Phys. (N. Y.) **23**, 390 (1963).

[2] T. Ericson, Phys. Letters **4**, 258 (1963).

[3] D. M. Brink and R. O. Stephen, Phys. Letters **5**, 77 (1963).

[4] L. Colli, I. Iori, M. G. Marcazzan, and M. Milazzo, Nucl. Phys. **43**, 529 (1963); E. Fort and P. Thouvenin, J. Physique **24**, 819 (1963); and M. Cadeau, D. Didier, B. Duchemin, G. Mouilhayrat, and P. Thouvenin, J. Physique **25**, 943 (1964).

[5] G. Andersson-Lindström, G. Betz, W. Mausberg, and E. Rössle, Mem. Soc. Roy. Sci. Liège **10**, 265 (1964).

ential cross-section measurements[6,7] of the reaction $C^{12}(C^{12},\alpha)Ne^{20}$, which has a spinless entrance channel and different spins of the excited states of Ne^{20}, have been very valuable in confirming the nuclear reaction concepts on which fluctuation theory is based. An additional simplification in this heavy-ion reaction is the large orbital angular momentum associated with both the C^{12} ions in the entrance channel and with the energetic alpha particles in the exit channels. This assures that the magnetic substates can be *independent* combinations of the angular momenta, and thus the damping of the fluctuations can be calculated simply from the number of these M states[7,8] allowed by angular-momentum considerations. Furthermore, as was confirmed by fluctuation analyses,[7,8] this heavy-ion reaction had the simplification of no detectable contribution of fast, direct-interaction processes.

It is clear that the $Al^{27}(\alpha,p)Si^{30}$ reaction does not have these simplicities. Even for protons to the 0-spin ground state of Si^{30}, the $\frac{5}{2}$ spin of Al^{27} and the $\frac{1}{2}$ spin of the proton allow several M values for angles other than 0° and 180°. However, the small orbital angular momenta of the outgoing protons and, to a lesser extent, of the incident alpha particles severely limit the effective number N_{eff} of M states that are independent. (The number N_{eff} is also called the fluctuation damping coefficient.[9]) The $Al^{27}(\alpha,p)Si^{30}$ reaction has the additional complication of direct interactions, which are expected to be more important because of the light particles in both the entrance and exit channels. Particularly at forward angles and for larger energies, the fraction of the reactions proceeding by direct interactions can be expected to be large. Under favorable conditions discussed in Sec. V, the number N_{eff} of M states damping the fluctuations can be determined, and the fraction y of direct interactions providing the remaining damping can then be determined.

Another important item in fluctuation analyses is the sample size. At the excitation energies involved, levels are completely unknown in regard to their energies, spins, and parities. Thus for a statistical analysis, a span of energy ΔE including many of these overlapping levels is needed. The magnitude of the sample size affects the accuracy with which values of the average cross section $\bar{\sigma}$, the coherence width Γ_0, the number N_{eff} of M states, and other quantities can be determined from the data. Almqvist *et al.*,[7] Hall,[9] and Böhning[10] have considered the uncertainties that arise from the finite size of the sample. (For example, Hall[9] notes that a sample size of 100 is required for a 20% accuracy in an experimental determination of the number $N_{\text{eff}}^{\text{exp}}$ of M states effective in the reaction.) Almqvist *et al.*[7] took the sample size to be the number ($S=\Delta E/\Gamma$) of coherence widths in the energy interval ΔE. More recently, however, Gibbs[11,12] has shown that the sample size applicable in these analyses is instead $n\approx(\Delta E/\pi\Gamma)+1$, and so the number of coherence widths required to obtain a desired accuracy is almost π times greater.[12a]

Fluctuations in the differential cross sections of many reactions have been measured with the experimental conditions required for a full analysis by fluctuation theory, namely, with energy resolutions finer than the coherence width and with the steps in the energies of measurement smaller than the coherence width Γ. For several studies,[5,7,13] the sample size $n=(\Delta E/\pi\Gamma)+1$ is less than 13; thus, appreciable corrections need to be applied to the results obtained from these analyses, and the uncertainties are correspondingly large.[11] For some studies[6,14,15] the sample size n was between 16 and 36, and so these results are subject to progressively smaller corrections and uncertainties. A sample size n of about 50 has been

---

[6] J. Borggreen, B. Elbek, and R. B. Leachman, Kgl. Danske Videnskab. Selskab, Mat. Fys. Medd. **34**, No. 9 (1964).

[7] E. Almqvist, J. A. Kuehner, D. McPherson, and E. W. Vogt, Phys. Rev. **136**, B84 (1964).

[8] J. Bondorf and R. B. Leachman, Kgl. Danske Videnskab. Selskab, Mat. Fys. Medd. **34**, No. 10 (1965).

[9] I. Hall, Phys. Letters **10**, 199 (1964).

[10] M. Böhning, in *Comptes Rendus du Congrès International de Physique Nucléaire* (Centre National de la Recherche Scientifique, Paris, 1964), Vol. II, p. 697 and also reported by T. Mayer-Kuckuk in the 1964 Hercegnovi Lectures (Max-Planck Institute report, Heidelberg, to be published).

[11] W. R. Gibbs, Phys. Rev. **139**, B1185 (1965).

[12] W. R. Gibbs, Los Alamos Scientific Laboratory Report LA 3266, 1965 (available from Clearing House for Federal Scientific and Technical Information, National Bureau of Standards, U. S. Department of Commerce, Springfield, Virginia).

[12a] *Note added in proof.* The sample size and its consequences have been discussed by M. Halbert and M. Böhning [Bull. Am. Phys. Soc. **10**, 120 (1965)] using methods similar to the ones employed here.

[13] M. L. Halbert, F. E. Durham, C. D. Moak, and A. Zucker, Nucl. Phys. **47**, 353 (1963); Y. Cassagnou, I. Iori, C. Levi, M. Mermaz, and L. Papineau, Phys. Letters **9**, 263 (1964); P. Strohal, P. Kulišić, Z. Kolar, and N. Cindro, Phys. Letters **10**, 104 (1964); E. Gadioli, G. M. Marcazzan, and G. Pappalardo, Phys. Letters **11**, 130 (1964); G. M. Temmer, Phys. Rev. Letters **12**, 330 (1964); L. Papineau, 1964 Hercegnovi Lectures (Centre d'Etudes Nucléaires de Saclay report, to be published); I. M. Naqib, R. Gleyvod, and N. P. Heydenburg, Nucl. Phys. **66**, 129 (1965); and R. E. Brown, J. S. Blair, D. Bodansky, N. Cue, and C. D. Kavaloski, Phys. Rev. **138**, B1394 (1965).

[14] B. W. Allardyce, W. R. Graham, and I. Hall, Nucl. Phys. **52**, 239 (1964); F. Rauch and E. Rössle, Phys. Letters **12**, 217 (1964); O. Häusser, P. von Brentano, and T. Mayer-Kuckuk, Phys. Letters **12**, 226 (1964); O. Häusser, A. Richter, P. von Brentano, and T. Mayer-Kuckuk, in *Comptes Rendus du Congrès International de Physique Nucléaire* (Centre National de la Recherche Scientifique, Paris, 1964), Vol. II, p. 728; O. Häusser, Inauguraldissertation, Erlangen University, 1964 (unpublished); A. A. Katsanos, H. K. Vonach, and J. R. Huizenga, Bull. Am. Phys. Soc. **9**, 667 (1964); M. L. Halbert, F. E. Durham, C. D. Moak, and A. Zucker in an extension of their measurements in Ref. 13 (private communication); G. G. Seaman, G. Dearnaley, W. R. Gibbs, and R. B. Leachman, Bull. Am. Phys. Soc. **10**, 156 (1965); G. G. Seaman, R. B. Leachman, and G. Dearnaley, *ibid.* **10**, 463 (1965). Also see Tandem-Laboratorium Jahresbericht 1964, Max-Planck Institute, Heidelberg (unpublished).

[15] P. von Brentano, J. Ernst, O. Häusser, T. Mayer-Kuckuk, A. Richter, and W. von Witsch, Phys. Letters **9**, 48 (1964); and T. Mayer-Kuckuk, J. Ernst, W. von Witsch, and P. von Brentano, in *Comptes Rendus du Congrès International de Physique Nucléaire* (Centre National de la Recherche Scientifique, Paris, 1964), Vol. II, p. 731.

covered[16] through the giant resonance region for $Al^{27}(p,\gamma)Si^{28}$. In the present $Al^{27}(\alpha,p)Si^{30}$ study, data giving a sample size of over 60 have been analyzed.

A distinct advantage of the use of the (α,p) reaction for fluctuation studies with particles is the ease with which measurements can be made at forward angles, including even 0° measurements. The fact that the particle in the exit channel is more penetrating than the particle in the entrance channel allows simple absorptive means of eliminating the forward scattered incident particles and even the beam itself. This principle has previously been used[6,7] for forward- and zero-angle measurements of the $C^{12}(C^{12},\alpha)Ne^{20}$ reaction. In the present case of $Al^{27}(\alpha,p)Si^{30}$ reactions, the forward angles are particularly interesting because the fraction of direct interactions at forward angles is likely to be appreciably greater than at back angles.

Another point of interest about the extreme forward angles, as well as the extreme back angles, is the change in the frequency distribution of cross section with angle. For 0° and 180°, angular momentum properties limit the number N_{eff} of M substates to one, and, for exclusively compound-nucleus reactions, fluctuation theory gives a χ^2 distribution with two degrees of freedom. This is a cross-section probability that decreases exponentially with cross section. For angles only a few degrees from 0° and 180°, the small admixture of other M states causes the probability of zero cross section to decrease to zero. Such changes are investigated in the present study.

Since data are readily obtained for protons to both the first-excited (2^+) and ground (0^+) states of Si^{30}, it is worthwhile to assess the relative significance of these two sets of data. Even for 0° and 180°, the number N_{eff} of effective M states is greater than one for protons to the excited states having spin, and so the change of the frequency distribution of cross section with angle is not expected to be great. Furthermore, the limiting number N of M states (for all M states independent and at an angle for which all M states have equal weight) is considerably greater for the reaction to the 2^+ state. This is seen from the relation[1]

$$N=(\tfrac{1}{2})(2s+1)(2I+1)(2s'+1)(2I'+1), \qquad (1)$$

which is valid for the present case of odd-A nuclei or particles. Unprimed quantities refer to the entrance channel and primed to the exit channel. For even-A nuclei or particles, the corresponding relation is[8]

$$N=\tfrac{1}{2}[(2s+1)(2I+1)(2s'+1)(2I'+1)+1]. \qquad (2)$$

This damping of fluctuations in the proton yield to the spin-2 state, even for 0° and 180°, due to the number N_{eff} of M states must be distinguished from the damping due to direct interactions if the fraction y of direct interaction is to be extracted from these fluctuation data. In our present high-spin case for Al^{27}, the M states are not independent, and so N_{eff} is not readily calculable. As is shown in Sec. V, the use of fluctuation analyses for reasonable determinations of both the number N_{eff} of M states and the fraction y of direct interactions requires that y be significantly different at forward and back angles with respect to the beam direction. Since this is not the case, determinations of N_{eff} and y for the excited state of the reaction being studied are not practical.

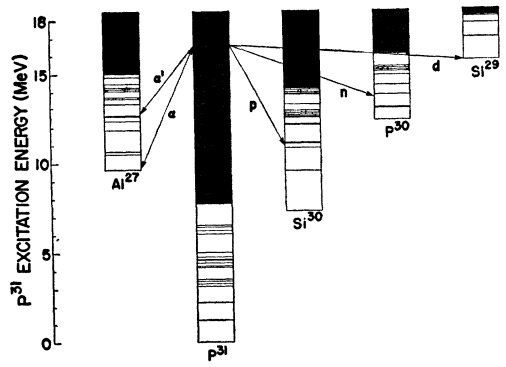

FIG. 1. Exit channels possible for the compound system P^{31}. The figure illustrates a typical excitation energy involved in the experiment. The level positions of some low-lying states of the nuclei are illustrated.

Comparison of the cross sections of protons to the ground and first excited states of Si^{30} indicates whether the compound nucleus at a given energy has many overlapping levels. If the product cross sections (normalized to have an average of unity) for the two exit channels are summed for all the energies measured and then properly normalized, the difference between this sum and unity is zero when the levels are completely overlapping and thus there are no isolated levels. This difference is proportional to the cross-correlation coefficient. (See Sec. IV.) Should the values of the cross-correlation coefficient center about zero for trials at various angles and for various energy spans ΔE of incident energy E, then mathematical assurance is provided that the fluctuations in the cross section are rarely, if ever, due to isolated levels of the compound nuclei. The large span of energies at each of the many angles measured in the present experiment allows ample test of the significance of cross correlations between these channels.

Figure 1 shows the various exit channels possible for the compound system P^{31}. The relative values of the lifetime of the compound state and of the recurrence time for returning to a given configuration of the compound state provide a measure of the sum of the exit probabilities[17] by the mnemonic

$$2\pi\langle\Gamma\rangle/\langle D\rangle=\sum T_l. \qquad (3)$$

[16] P. P. Singh, R. E. Segel, L. Meyer-Schützmeister, S. S. Hanna, and R. G. Allas, Nucl. Phys. (to be published).

[17] J. M. Blatt and V. F. Weisskopf, *Theoretical Nuclear Physics* (John Wiley & Sons, Inc., New York, 1952), p. 386.

With a knowledge of the transmission coefficients T_l for each of the various exit channels energetically possible in Fig. 1, the width-to-spacing ratio $\langle\Gamma\rangle/\langle D\rangle$ can be calculated. The fact that $\langle\Gamma\rangle/\langle D\rangle$ is found to be greater than one confirms the overlapping of levels[18] and indicates that a central value of zero for the cross-correlation functions should be expected. For this width-to-spacing ratio calculation, the transmission coefficients in Fig. 2 were determined from optical model calculations with the potential-well parameters taken from Huizenga and Igo[19] for alpha particles, from Perey[20] for protons, and from Bjorklund and Fernbach[21] for neutrons.

Use of these transmission coefficients T_{lj} also makes possible calculations of the ensemble-averaged, compound-nucleus cross sections for reactions proceeding through each of the separate M states. The scattering from channel α to channel β proceeding through a given M substate μ (μ denotes the set of magnetic quantum numbers, $\{s_z,I_z,s_z',I_z'\}$) is given by[22]

$$\bar{\sigma}_\mu{}^{\alpha\beta}(\theta)=k_\beta{}^2\sum_{J,\pi}\frac{\sigma_c{}^\alpha(s_z,I_z,J,s_z+I_z,\pi,0)\sigma_c{}^\beta(s_z',I_z',J,s_z+I_z,\pi,\theta)}{\sum_{\gamma,s_z',I_z}k_\gamma{}^2\int d\Omega\sigma_c{}^\gamma(s_z',I_z',J,s_z+I_z,\pi,\theta)},\tag{4}$$

where the capture cross section σ_c is

$$\sigma_c{}^\gamma(s_z,I_z,J,\pi,\theta)=\frac{4\pi^2}{k_\gamma{}^2}\sum_{l,m,j,j_z}[C(l,m,s,s_z;j,j_z)C(I,I_z,j,j_z;J,J_z)]^2|Y_l{}^m(\theta,\varphi)|^2T_{lj}{}^\gamma.\tag{5}$$

Here, $T_{lj}{}^\gamma$ is the transmission coefficient in the generalized exit channel γ and k_γ is the wave number in channel γ. The symbol π denotes the parity of the compound state, C a Clebsch-Gordan coefficient, and $Y_l{}^m$ a spherical harmonic.

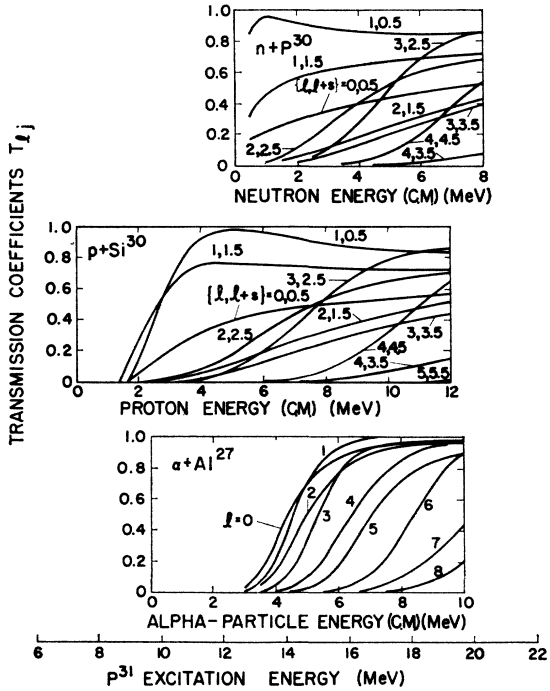

FIG. 2. Transmission coefficients $T_{lj}{}^\gamma$ calculated by the optical model for various exit channels γ. Abscissas are displaced to the common excitation energy of the compound system P^{31}. Optical model parameters were from Ref. 19 for alpha particles, from Ref. 20 for protons, and Ref. 21 for neutrons.

This method in Eqs. (4) and (5) is equivalent to that employed previously[8,23] for the case of zero spins. The constituent cross sections $\sigma_\mu{}^{\alpha\beta}(\theta)$ are called *basic cross sections* and individually are expected to have a frequency distribution that is a χ^2 distribution with two degrees of freedom. The γ sum in the denominator in Eq. (4) is over all exit channels (particles and excitation energies of residual nuclei). For the Hauser-Feshbach calculations used in this work, an adequate summation over the exit channels γ included only the first 30 excited levels of Si^{30} populated by proton exit channels, the first six excited levels of P^{30} populated by neutron exit channels, and the first six excited levels of Al^{27} populated by alpha-particle exit channels.

Bondorf and Leachman[8] show that the effective number $N_{\rm eff}{}^{\rm HF}$ of M states calculated from the Hauser-Feshbach cross sections of (4) is

$$N_{\rm eff}{}^{\rm HF}=[\sum_\mu\bar{\sigma}_\mu(\theta)]^2/\sum_\mu[\bar{\sigma}_\mu(\theta)]^2,\tag{6}$$

which assumes that all the basic cross sections $\sigma_\mu(\theta)$ are independent. Similarly, the experimental value of the effective number $N_{\rm eff}{}^{\rm exp}$ of M states is determined[8] by using the measured cross sections in

$$N_{\rm eff}{}^{\rm exp}=\frac{\langle\sigma(\theta)\rangle^2}{\langle[\sigma(\theta)]^2\rangle-\langle\sigma(\theta)\rangle^2}.\tag{7}$$

[18] P. A. Moldauer, Phys. Letters 8, 70 (1964). This letter discusses the effects of a finite value of the width-to-spacing ratio Γ/D. At all our energies, with the possible exception of the lowest energy where $\Gamma/D\approx4$, these effects are insignificant and so were neglected.

[19] J. R. Huizenga and G. Igo, Nucl. Phys. **29**, 462 (1962); and Argonne National Laboratory Report No. ANL 6373, 1961 (unpublished).

[20] F. G. Perey, Phys. Rev. **131**, 745 (1963).

[21] F. Bjorklund and S. Fernbach, Phys. Rev. **109**, 1295 (1958).

[22] W. Hauser and H. Feshbach, Phys. Rev. **87**, 366 (1952).

[23] E. W. Vogt, D. McPherson, J. Kuehner, and E. Almqvist, Phys. Rev. **136**, B99 (1964).

When a small number of orbital angular momenta are involved, one expects a lower value for $N_{\text{eff}}^{\text{exp}}$ compared to $N_{\text{eff}}^{\text{HF}}$ as a consequence of the lack of independence of the basic cross sections. However, previous comparisons have been made for conditions where the limiting N value from Eq. (1) or Eq. (2) was not greater than the maximum orbital angular momenta involved, and $N_{\text{eff}}^{\text{exp}} \approx N_{\text{eff}}^{\text{HF}}$ resulted.[8,15] In the present higher spin case, $I=\frac{5}{2}$ results in a larger $N=6$ value for the limiting number of magnetic substates than the maximum orbital angular momentum $l_{\max}$ obtained from the T_l values in Fig. 2. Thus, $N_{\text{eff}}^{\text{exp}} < N_{\text{eff}}^{\text{HF}}$ is possible.

An experimental determination of $l_{\max}$ is provided by comparing at different angles the excitation functions for a particular exit channel. Since the differential cross sections being studied can be expressed in terms of a finite number of partial waves, the statistical combination of these waves can be expected to lead to an angular cross correlation function. Brink *et al.*,[24] show that the data should be correlated over an angular interval of $\alpha \equiv \theta_1 - \theta_2 \approx 1.8/l_{\max}$, where the angles are expressed in radians.

II. EXPERIMENTAL PROCEDURE

The equipment shown schematically in Fig. 3 for measurement of excitation functions at forward angles was installed in a 10-in.-diam scattering chamber of the Los Alamos 8.5-MV Van de Graaff accelerator. A beam of He^4 particles was collimated by a $\frac{1}{8}$-in. gold aperture C to fall on a thin target T of self-supporting aluminum. Beam collection for current integration was made in a copper block F, which was mounted on a large aluminum plate, from which it was insulated electrically by nylon screws and a thin film of Teflon. A gold ring suppressor S, maintained at -300 V with respect to the chamber, prevented secondary electrons from entering or leaving the beam collector. The collector itself was lined with platinum foil to reduce background reaction processes, and at its rear face on the axis of the beam a $\frac{5}{32}$-in. aperture A was provided in a gold sheet H, which was adequate in thickness to stop the most energetic protons from the target ($\approx$11 MeV). The aperture was covered by a thin absorber intended to stop the He^4 particles incident upon it, but to allow the higher energy proton groups to penetrate with minimum energy loss, and so to enter the 0° detector. We consider in detail below some of the problems of choosing a material suitable for this absorber.

Figure 3 shows also the arrangement of four semiconductor detectors D as used for studying the excitation function at forward angles. All four detectors were 3-mm deep, 80-mm^2 area lithium-drifted silicon surface-barrier detectors (supplied by Technical Measurement

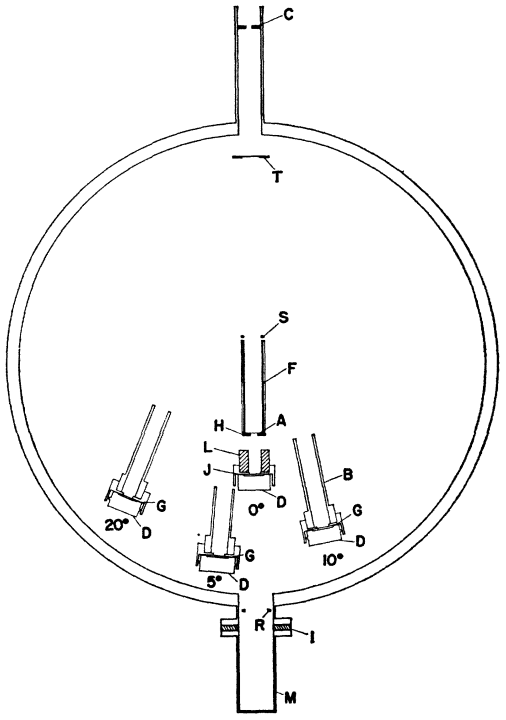

FIG. 3. Experimental arrangement used to measure the excitation functions at forward angles. See the text in Sec. II for details.

Corporation). These were cooled to about 5°C by being mounted on the same aluminum plate as the beam collector. This plate was cooled by a chilled water flow. The 0° detector was fitted with a lead collimator L to reduce the area that could receive gamma rays from the beam absorber and was placed sufficiently close that outscattering of protons by the beam absorber was negligible. The exposed area of the detector, $\frac{1}{4}$ in. in diameter, was covered with a thin (5×10^{-5} in.) nickel foil to exclude light. The other three detectors, at 5°, 10°, and 20°, were fitted with brass collimation tubes B to prevent scattered protons from entering the detectors. The four detectors were mounted radially with respect to the target at required angles on the cooled aluminum plate. All detectors except the 0° detector were covered with 0.001-in.-thick gold absorbers G to exclude scattered alpha particles and light. The apertures of these detectors were $\frac{1}{4}$ in., which at an average radius of 7 in. corresponds to an angular acceptance of about 2°; analysis of the experimental results has shown that this is adequately small in comparison with the coherence angle, found to be about 20°. Excitation function measurements at 30°, 40°, and 50° were made with a geometry similar to that in Fig. 3, but with the beam collector F removed and with beam collection in the insulated cup M behind the insulation I. In this case, secondary electron suppression was achieved by the insulated ring R.

For excitation function measurements at back angles,

[24] D. M. Brink, R. O. Stephen, and N. W. Tanner, Nucl. Phys. 54, 577 (1964).

between 140° and 175°, the target was moved so as to be symmetrically near the exit of the chamber. Again, the beam collector F was removed and beam collection was made by means of the insulated cup M. In this case, the plate holding the detectors was rotated through 180° with respect to its former position.

Angular distributions were measured in a more conventional manner with the target at the center of the chamber and the four counters at 21° spacings on a single movable arm. In this arrangement, the counters had a 0.5-in.-diam. aperture and were at a radius of 3.9 in.

Four charge-sensitive preamplifiers at the scattering chamber amplified the signals, which were fed into a pair of RIDL universal temporary storage accessory units (Model 52-30) for routing into four memory subgroups of a RIDL 400-channel pulse-height analyzer. In each run, after a predetermined charge was accumulated at the beam collector (as measured by a current integrator), the analyzer memory was punched on paper tape. The data were subsequently converted to magnetic tape storage and analyzed by an IBM-7094 computer by means of two consecutive programs. In the first, peaks in the proton spectra were located if above a certain minimum count chosen to eliminate false peaks arising from statistical fluctuation of the number of counts per channel. These peak positions could then be plotted in order to reveal gain changes, detector resolution, contaminant reactions, etc. A typical proton spectrum taken at 140° detector angle and 7.535-MeV He^4 energy is shown in Fig. 4. Clearly, the ground and first-excited state groups are well resolved, but resolution of other groups is inadequate. When the widths of the peaks were established and the gains normalized, the second computer program was applied to sum the counts within the ground and first-excited state peaks.

A correlation function analysis[2,3] of the first samples of data, taken with an aluminum target about 100 $\mu g/cm^2$ in thickness, showed that the experimental energy resolution was inadequate. The apparent coherence width Γ was essentially the same as the energy resolution. Thinner targets were tried until analyses showed coherence widths appreciably greater than the experimental resolutions for all the incident alpha-particle energies. This led to a choice of target thickness of the order of 10 $\mu g/cm^2$, which gave an energy resolution of approximately 5 keV. The targets were prepared as self-supporting films by vacuum evaporation onto a soluble substrate followed by stripping on a water surface. A number of such targets were used throughout the experiment, and their relative thicknesses were calibrated by a series of runs over the same energy range with pairs of targets. Energy ranges were chosen for this such that the yield was high and reasonably constant. (A 30-$\mu g/cm^2$ target with a 45° orientation to the beam, which resulted in a target thickness about twice the coherence width Γ, was used for angular distribution measurements.)

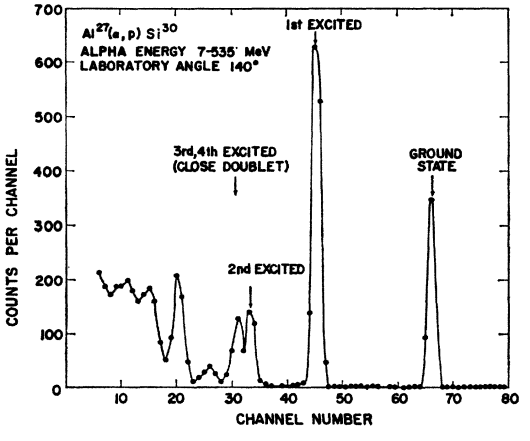

FIG. 4. A proton spectrum from the reaction $Al^{27}(\alpha,p)Si^{30}$ taken at 140° detector angle and $E_\alpha = 7.535$ MeV.

The energy spread of the Van de Graaff beam had previously been measured to be less than 1.3 keV.

Once the target thickness was decided, the integrated charge for each cross-section determination was chosen in terms of the statistical accuracy required in the proton count. Mean counts of more than 100 protons were recorded for each datum point. The counting statistics then resulted in uncertainties[12,25] in the coherence widths and other quantities of interest that were considerably less than the uncertainties arising from the sample size.

The beam current allowable in the forward angle studies was restricted by the behavior of the thin absorber at the rear of the beam collector. Some difficulty was experienced in finding a suitable material subject to the following requirements:

(1) The foil must be thin and uniform, just thick enough to stop the most energetic He^4 particles used.

(2) The foil must not itself be a source of (α,p) reactions that could lead to a background in the 0° detector. Since the absorber is so much thicker and closer to this detector than is the aluminum target, the requirement on chemical purity is severe.

(3) The foil must not undergo mechanical rupture under the effect of the beam bombardment employed or the 0° detector may be rapidly damaged. The poor heat transfer from a thin (0.001-in.) foil requires the use of high melting-point materials.

Gold and platinum, although satisfactory in other respects, tended to melt at current densities corresponding to about 60 W/cm^2. Tantalum and tungsten contained troublesome impurities and moreover showed grain boundary embrittlement that resulted in fracture of the foil between two of the grains which had grown under bombardment. Molybdenum was found to be

[25] H. L. Acker, Max-Planck Institute Bericht, Heidelberg, 1964IV13 (unpublished).

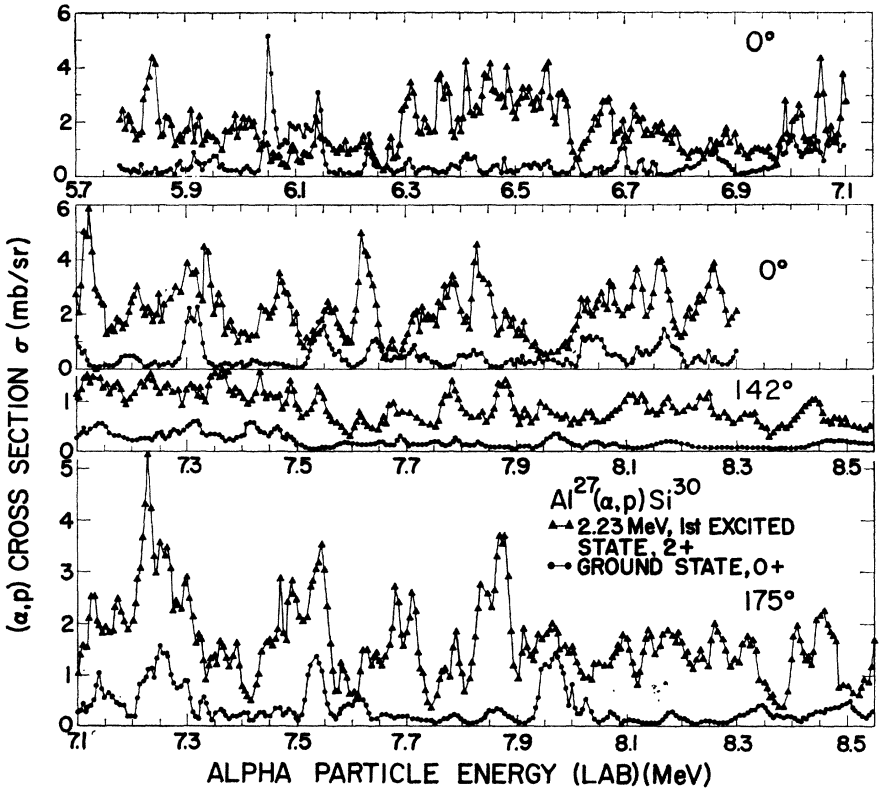

FIG. 5. Excitation functions for three of the eleven angles measured. The data shown have been corrected (see Sec. III) for the energy spreads of the Van de Graaff and introduced by the target thickness. Data were taken at energy increments δ of 5 keV.

free from this effect, but was usually too impure; some samples contained appreciable aluminum as an impurity. Other samples (from the same supplier) were found to be relatively free from contamination. Beam currents of about 1 μA could be used safely with molybdenum absorbers and about 0.5 μA with platinum absorbers. In the measurements at other angles no thin absorber for the beam was required, and the beam current was limited by other factors, such as the count rate in the pulse-height analyzer. The aluminum targets withstood beam currents of 2.5 μA without deterioration.

III. EXPERIMENTAL RESULTS

The $Al^{27}(\alpha,p)$ yield to the ground and first-excited states of Si^{30} was measured at a total of eleven angles through ranges of bombarding energy as follows: 0°, 5°, 10°, and 20° for 5.78 MeV through 8.30 MeV; 30°, 40°, and 50° for 7.25 MeV through 8.10 MeV; 140°, 165°, 170°, and 175° for 7.10 MeV through 8.55 MeV. A few of these excitation functions are shown in Fig. 5. Cross-section measurements were made in 5-keV intervals, δ, of bombarding energy, which is a smaller step than the lowest coherence width determined from the results, and comparable with the experimental energy resolution.

A small correction for experimental resolution was made to the data before fluctuation analyses were performed. The spread in Van de Graaff energy and the energy loss in the target were assumed to result in a bombarding energy distribution that was rectangular with a full width ρ. This resolution can be removed if a parabolic fitting of three neighboring energy points of the true excitation function $\sigma(E)$ is assumed to be an accurate representation of the cross section between these points. Then the resulting experimental excitation function $\tilde{\sigma}(E)$ for either differential or integrated cross sections can readily be shown to be

$$\tilde{\sigma}(E)=\sigma(E)+(\rho^2/24)\sigma''(E), \tag{8}$$

which, for these conditions, results in the equivalent equation

$$\tilde{\sigma}(E)=\sigma(E)+(\rho^2/24)\tilde{\sigma}''(E). \tag{9}$$

The double prime denotes the second derivative. Thus the data shown in Fig. 5 and all the data used in analyses have been corrected for resolution by subtracting $\rho^2\tilde{\sigma}''(E)/24$ from the experimental data.[26]

The angular distributions at the much larger 0.2-MeV steps of bombarding energy between 5.8 and 7.0 MeV are shown in Fig. 6 for the ground-state reaction and in Fig. 7 for the first excited state. The results from least squares fits of the series $\sigma(\theta)=\sum a_\nu P_\nu(\cos\theta)$

[26] D. W. Lang, Nucl. Phys. (to be published) similarly considers the effects of experimental resolution. Also see D. W. Lang, Bull. Am. Phys. Soc. 9, 461 (1964).

TABLE I. Coefficients a_ν for the least-squares fits of the Legendre polynomial sum $\sigma(\theta)=\sum a_\nu P_\nu(\cos\theta)$ to the angular distributions in Figs. 6 and 7.

E_α (MeV)	a_0	a_1	a_2	a_3	a_4	a_5	a_6
				Ground state			
5.8	0.743±0.007	0.211±0.011	−0.093±0.014	−0.180±0.016	−0.209±0.019	−0.154±0.019	0.000±0.021
6.0	0.956±0.018	−0.274±0.023	−0.752±0.034	0.194±0.041	−0.054±0.046	−0.071±0.057	0.112±0.059
6.2	0.305±0.004	−0.059±0.006	0.000±0.007	0.050±0.009	−0.145±0.011	−0.013±0.010	0.010±0.011
6.4	0.525±0.014	0.173±0.020	−0.052±0.026	−0.068±0.032	−0.120±0.036	0.037±0.036	0.068±0.040
6.6	1.095±0.019	0.144±0.026	−0.552±0.037	0.139±0.042	−0.152±0.050	−0.279±0.044	−0.179±0.049
6.8	0.501±0.007	−0.064±0.011	−0.011±0.015	−0.198±0.017	−0.091±0.020	0.091±0.020	−0.044±0.022
7.0	0.665±0.025	0.093±0.040	0.032±0.050	0.244±0.060	−0.034±0.069	0.052±0.074	0.127±0.082
				First excited state			
5.8	1.702±0.022	0.310±0.034	0.515±0.045	−0.054±0.052	0.208±0.061	0.052±0.064	−0.047±0.071
6.0	2.161±0.040	−0.832±0.064	0.581±0.079	−0.099±0.099	−0.393±0.117	0.082±0.141	−0.023±0.149
6.2	1.730±0.021	0.032±0.033	0.414±0.043	−0.263±0.050	−0.128±0.059	−0.124±0.061	0.011±0.068
6.4	2.833±0.031	−0.901±0.047	0.513±0.061	0.258±0.072	−0.158±0.084	0.058±0.086	−0.012±0.095
6.6	4.036±0.052	−0.680±0.080	0.786±0.105	−0.564±0.123	0.009±0.144	−0.640±0.148	0.068±0.164
6.8	3.009±0.025	−0.382±0.039	0.759±0.051	−0.425±0.059	−0.170±0.069	−0.058±0.072	−0.278±0.080
7.0	2.029±0.033	0.369±0.051	0.202±0.066	−0.152±0.077	−0.234±0.090	−0.229±0.092	−0.191±0.101

of Legendre polynomials to these angular distributions is given in Table I. The fact that only low orders of ν are required agrees with the small orbital angular momenta expected from the transmission coefficients in Fig. 2. The need for odd orders of Legendre polynomials confirms that reactions observed for this energy resolution, which was about twice the coherence width Γ, proceed through more than one state with different values of total angular momentum J.

IV. FLUCTUATION ANALYSES

A. Definitions

We define x to be the cross section divided by the average cross section in the range ΔE being considered. Thus, for either differential or integral cross sections, $x\equiv\sigma(E)/\langle\sigma(E)\rangle$. Then we may define the autocorrelation function

$$R(\epsilon)\equiv\delta(\Delta E-\epsilon)^{-1/2}\sum_{E_i=E_{\min}}^{E_i=E_{\min}+\Delta E-\epsilon}[x(E_i)-1]\times[x(E_i+\epsilon)-1] \quad (10)$$

used in the following analyses. Here, δ is the energy increment between data points. With this definition, the fluctuations in $R(\epsilon)$ for $\epsilon\gg\Gamma$ have a constant variance, which is[27]

$$R^2(0)[\tan^{-1}S-(2S)^{-1}\ln(1+S^2)]/S. \quad (11)$$

For $\epsilon\ll\Delta E$, Ericson[1] has shown

$$R(\epsilon)=\frac{R(0)}{1+\epsilon^2/\Gamma^2}. \quad (12)$$

For the determinations reported in this paper, the coherence width Γ is extracted by a fit of Eq. (12) to the ratio of $R(0)$ to $R(\delta)$, where both are obtained from using the data in Eq. (10). With $R(0)$ or Γ so obtained from Eq. (10), the expression (11) for the variance of the fluctuations in $R(\epsilon)$ provides an alternative determination of the other (since $S=\Delta E/\Gamma$).

Stephen[28] has shown that the value of $R(0)$ provides information about the amount of direct interaction and the fluctuation damping coefficient N by means of

$$R(0)=(1-y^2)/N, \quad (13)$$

where y is the fraction of the cross section which proceeds by direct reaction. Equation (13) is a restricted form of

$$R(0)=(1-y^2)/N_{\rm eff}^{\rm HF}+2y(1-y)\sum_{\mu=1}^{N}\beta_\mu\gamma_\mu, \quad (14)$$

which is obtained from considerations of the generalized frequency distributions.[12] Here, β_μ and γ_μ are defined for a given M substate μ by

$$\beta_\mu=\bar\sigma_\mu^{\rm CN}(\theta)/[\sum_\mu\bar\sigma_\mu^{\rm CN}(\theta)] \quad (15)$$

and

$$\gamma_\mu=\sigma_\mu^{\rm DI}(\theta)/[\sum_\mu\sigma_\mu^{\rm DI}(\theta)], \quad (16)$$

where the superscripts denote compound nucleus and direct interaction. Since the values of β_μ and γ_μ are determined primarily by angular-momentum considerations, we expect that $\beta_\mu\approx\gamma_\mu$, and hence

$$(N_{\rm eff}^{\rm HF})^{-1}=\sum_{\mu=1}^{N}\beta_\mu^2\approx\sum_{\mu=1}^{N}\beta_\mu\gamma_\mu, \quad (17)$$

where the equality follows from Eq. (6) and the ap-

[27] This expression results from the assumption that the average over the experimentally determined cross section is identical to the ensemble averaged cross section; hence this expression is approximate.

[28] R. O. Stephen, thesis, University of Oxford, 1963 (unpublished)

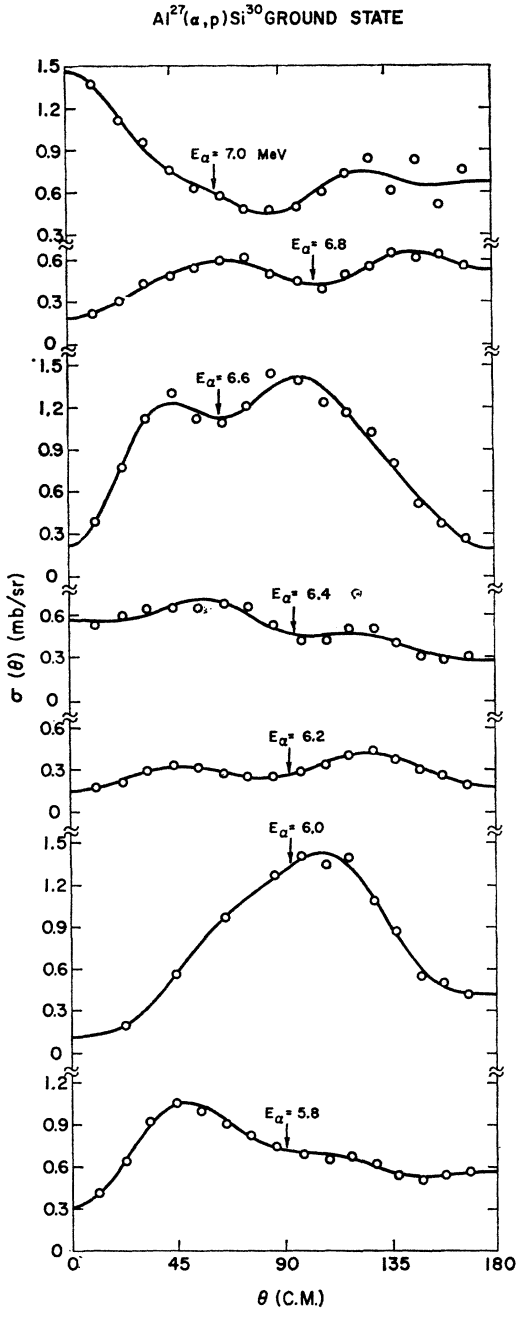

FIG. 6. Angular distributions for the reaction to the ground state of Si^{30}. Curves are least-squares fits of a Legendre polynomial sum to the data. Coefficients for the fit are given in Table I.

proximation is close. Substituting the second part of Eq. (17) into Eq. (14) leads to Eq. (13) with N replaced by $N_{\text{eff}}^{\text{HF}}$. A trial calculation using Hauser-Feshbach determinations of β_μ and distorted-wave Born approximation determinations of γ_μ verifies Eq. (17) to within 5% for all angles for the present reaction.

We also define a cross-correlation function for data sets 1 and 2 by

$$C_{12}(\epsilon)=\delta[\Delta E(\Delta E-\epsilon)R_1(0)R_2(0)]^{-1/2} \times \sum_{E_i=E_{\min}}^{E_i=E_{\min}+\Delta E-\epsilon} [x_1(E_i)-1][x_2(E_i+\epsilon)-1] \quad (18)$$

for $\epsilon\geq 0$; similarly, $C_{12}(-\epsilon)=C_{21}(\epsilon)$ for $\epsilon<0$. The quantities $R_1(0)$ and $R_2(0)$ are the corresponding autocorrelation functions for zero argument.

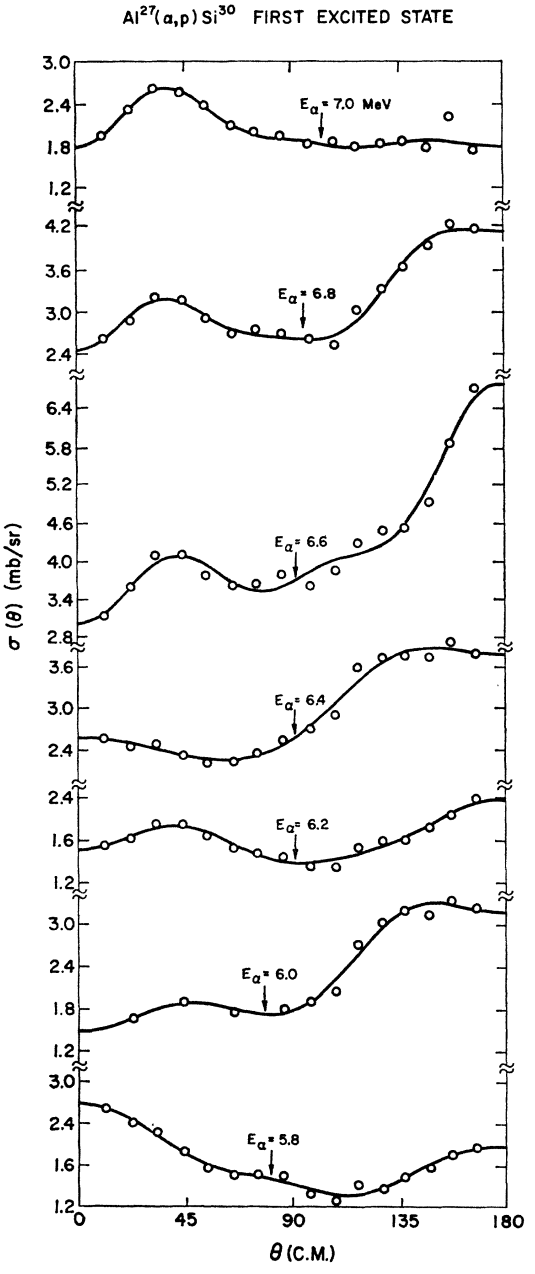

FIG. 7. Angular distributions for the reaction to the first-excited state of Si^{30}. Curves are least-squares fits of Legendre polynomials to the data. Coefficients for the fit are given in Table I.

B. Effects of Finite Sample Size

Since the present data provide a large sample size, we may study corrections applicable to a small sample by the following method. First, the data are analyzed as a whole; second, the data are separated into two parts and each section analyzed, and the quantity of interest obtained from each section is averaged; third, the data are separated into three parts, etc. If the entire range of data contains S coherence widths, it is argued in the following paper[11] that the number of independent points n is given by

$$n\approx(S/\pi)+1. \tag{19}$$

The full range of the data has n independent points, the half range has $n/2$ independent points, etc. Thus, experimentally determined quantities are obtained as a function of sample size n, and these may be compared with the theoretical predictions.

We now analyze the data in terms of $R_0(0)$ and Γ for the sample size effect. Figure 8 shows the points for $R_0(0)$ obtained by the process of splitting the 175° data of the ground-state reaction into sample sizes n. The solid curve is the relation[11,12]

$$R(0)=\frac{(n-1)(4n-3)}{4n^2} \tag{20}$$

for the autocorrelation $R(0)$ expected for a sample size n when $N=1$. Comparison between the expected coherence width Γ and the true coherence width Γ_0 similarly obtained from sample sizes n of the 175° data of the ground-state reaction is made in Fig. 9. The curve

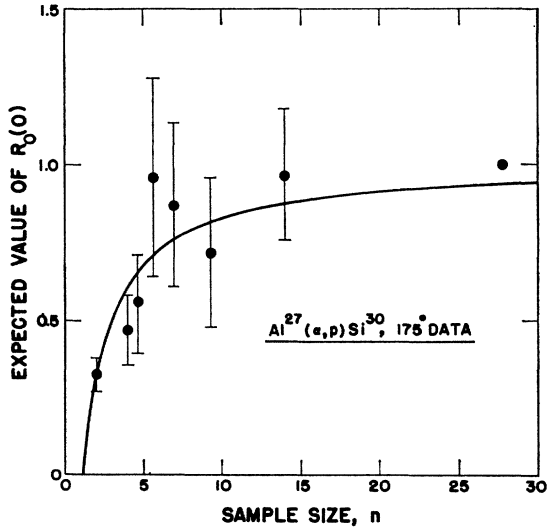

FIG. 8. Sample size effects on the autocorrelation function $R(0)$. Points are of the ground-state data for 175° shown in Fig. 5. Data were analyzed for $R_0(0)$ in sections with the indicated sample sizes n and then averaged. The solid curve is calculated from Eq. (20), and the uncertainties were obtained by the method of Ref. 11.

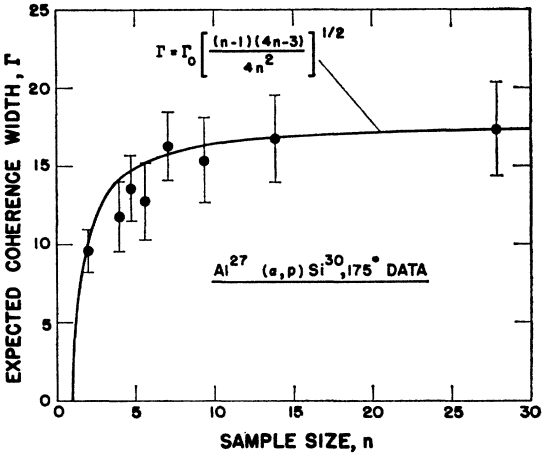

FIG. 9. Sample size effects on the coherence width Γ. Points are from the ground-state data for 175° shown in Fig. 5. Data were analyzed for Γ in sections with the indicated sample sizes n and then averaged. Uncertainties were obtained from the sample sizes n by the method of Ref. 11.

for the expected[11,12] coherence width Γ is

$$\Gamma=\Gamma_0\left[\frac{(n-1)(4n-3)}{4n^2}\right]^{1/2}, \tag{21}$$

with Γ_0 taken to be 18 keV. Agreements between the sample size theories of Eqs. (20) and (21) and the correlation coefficient and coherence width data in Figs. 8 and 9, respectively, are satisfactory.

We now make use of the procedure to determine the effective number $N_{\text{eff}}^{\text{exp}}$ of M states even in the presence of nonstationary effects. Data are considered for which $y=0$, as is considered to be the case for all back angles. Since the data extend over a wide range of energy, the average cross section is not constant, or, in statistical language, the process is not stationary.

If N_{eff} is assumed to be a constant, its value can be obtained without the uncertainty of dividing the cross section by a calculated moving average. It has been shown[12] that, as long as the process is stationary,

$$N_{\text{eff}}R(0)\approx\frac{(n-1)(4n-4+N_{\text{eff}})}{4n^2}, \tag{22}$$

for $N_{\text{eff}}=1$, 2, and 3. Equation (22) predicts a straight line with slope $(N_{\text{eff}}^{\text{exp}})^{-1}$ from a plot of $R-(n-1)/4n^2$ against $[(n-1)/n]^2$. For very small segments of the data, the process must be stationary, so that the slope of such a curve near the origin gives a good estimate of $(N_{\text{eff}}^{\text{exp}})^{-1}$. In a fit to the data thus divided into sectors of equal sample size n and averaged, the fit is principally determined by the points with small sample size n as a result of their greater number. In the upper part a of Fig. 10, such a plot is made for the 175° data of the ground-state reaction, for which $N_{\text{eff}}^{\text{exp}}$ is ex-

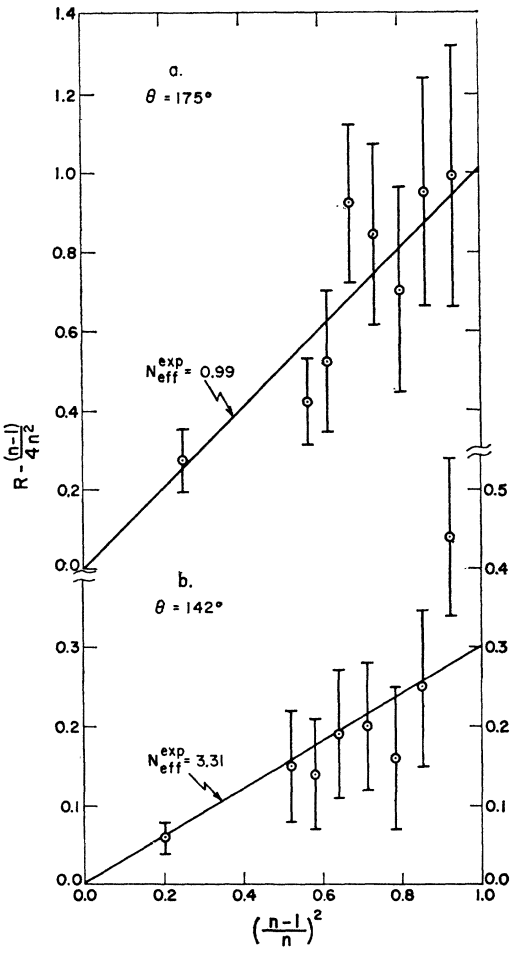

FIG. 10. Determination of the effective number $N_{\text{eff}}^{\text{exp}}$ of M states applicable to the ground-state data of 175° and 140°. Data shown in Fig. 5 were analyzed in sections with sample size n and then averaged. The points farthest to the right correspond to the full range of the data, the next to the right correspond to two halves, the next correspond to three thirds, etc. The points farthest to the left correspond to fourteen fourteenths of the full range of the data. Least-squares fits to Eq. (22) are used to determine $N_{\text{eff}}^{\text{exp}}$.

pected to be only slightly greater than one. A least-squares fit to all of the points gives $N_{\text{eff}}^{\text{exp}}=0.99$. The deviation from a straight line for a large sample is not evident in this figure, but appears in the similar analysis in the lower part *b* of Fig. 10 for the 140° (142° center-of-mass) data. Here, the linear relation of Eq. (22) is evident only for less than half of the full sample size, and so a nonstationary process is perhaps indicated.

C. Results

The above types of analyses were carried out over different energy regions for different purposes. The various regions and the results obtained in each are as follows.

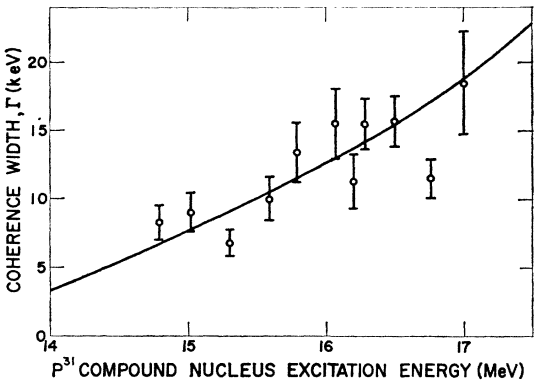

FIG. 11. Variation of the coherence width Γ with energy. These widths were determined from data at all angles for both ground and first-excited state reactions. The widths obtained from the use of the autocorrelation functions of Eq. (12) were corrected for finite sample size by the use of Eq. (21). Uncertainties were obtained from the sample sizes n by the method of Ref. 11. The solid curve is a statistical model calculation normalized to the coherence width results.

1. Small Energy Steps for All Angles

The data were broken into sections of about 300 keV in size, and autocorrelation functions were calculated for each section for all angles. The values of y obtained from these small sections by Eq. (13) were found to be too uncertain to be useful individually, but the extracted values for Γ do have significance. This is due partly to the fact that the relative error in Γ is only slightly more than one-half the error in $R(0)$ and partly to the fact that Γ can logically be averaged over different angles. Moreover, the variation of y with angle prohibits such an averaging. The results for Γ as a function of excitation energy are shown in Fig. 11. The solid curve is the result of a statistical model calculation based on currently accepted parameters with somewhat arbitrary normalization.

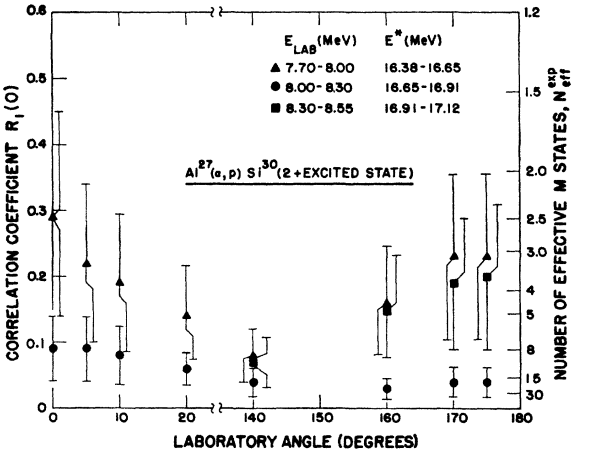

FIG. 12. Values of $R_1(0)$ from autocorrelation function analyses of the first-excited-state data of three neighboring sections of energy. The lower values for the 8.0- to 8.3-MeV data indicate possible intermediate structure effects in this region of energy.

One exception may be noted with regard to the significance of $R(0)$. In the region from 8.0- to 8.3-MeV bombarding energy for the reaction leading to the first excited state, $R_1(0)$ is anomalously small and nearly constant over all angles. These results are plotted in Fig. 12 along with $R_1(0)$ results for the corresponding data of the neighboring energy sectors. The damping accounting for the lower $R_1(0)$ values in this 8.0- to 8.3-MeV region might be an indication of a nonstatistical behavior (as some sort of intermediate resonance).[29,30]

2. *Large Energy Steps for All Angles*

It is assumed that there is no direct reaction in the back-angle ($\geq 140°$) data for protons to the ground state. Distorted-wave-Born approximation calculations indicate that the direct-interaction cross section in this region is at most 20% of the greatest direct-interaction cross section at forward angles. Thus only if the fraction of direct reaction y at forward angles is very large need we be concerned about this assumption. For example, 90% direct reaction at this angle of greatest cross section would then cause only $\leq 4\%$ error in the N_{eff} determination at the corresponding back angle. In the next Sec. (IV C 3), the fraction of direct reaction at forward angles is shown to be $<60\%$. An alternative justification of the $y=0$ assumption for back angles is provided in Sec. V by the method of compound-nucleus fore-aft symmetry.

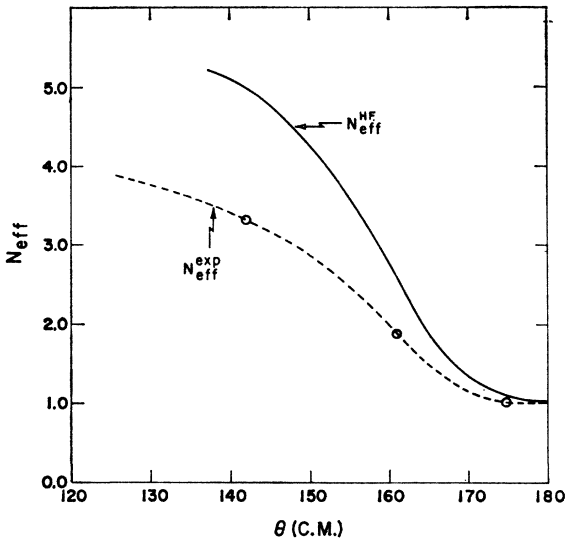

FIG. 13. Comparison of the experimental number $N_{\text{eff}}^{\text{exp}}$ and the calculated number $N_{\text{eff}}^{\text{HF}}$ of M states. The smaller value of $N_{\text{eff}}^{\text{exp}}$ is attributed to the lack of independence between M states. The dotted line arbitrarily drawn through the $N_{\text{eff}}^{\text{exp}}$ points is used for the true value of N_{eff} at these and π-θ angles.

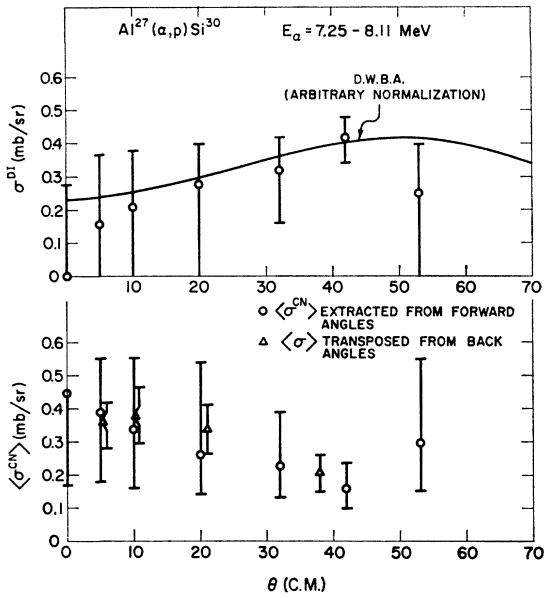

FIG. 14. The direct-interaction and compound-nucleus cross sections determined by the analysis of Sec. IV C2. The distorted-wave-Born-approximation calculation was made with an $l=2$ angular-momentum transfer.

If the fraction y of direct interactions is taken to be zero at back angles, then the value of $N_{\text{eff}}^{\text{exp}}$ for these angles can be extracted as indicated in Sec. IV B. These results together with a transmission coefficient calculation of $N_{\text{eff}}^{\text{HF}}$ are shown as a function of the angle θ in Fig. 13. The true values of N_{eff} are hereafter assumed to be those read from the arbitrarily drawn dashed line through the $N_{\text{eff}}^{\text{exp}}$ points. Since N_{eff} must be symmetric about 90°, these may be applied to the π-θ forward angles to allow the determination of the direct-reaction part of the cross section. The values of y multiplied by the average cross section give the direct-interaction cross section, and if this is subtracted from the energy-averaged cross section the energy-

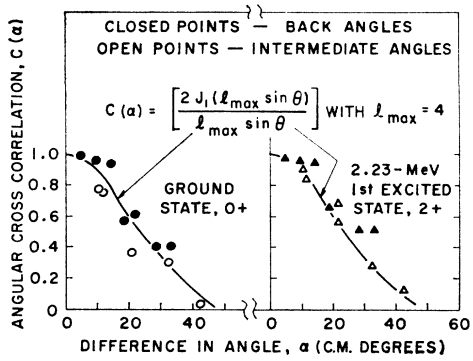

FIG. 15. Angular cross correlation functions $C_0(\alpha)$ and $C_1(\alpha)$ for the angular differences α for the 7.25- to 8.11-MeV data. The cross correlations were calculated from Eq. (18).

[29] K. Izumo, Progr. Theoret. Phys. (Kyoto) **26**, 807 (1961); B. Bloch and H. Feshbach, Ann. Phys. (N. Y.) **23**, 47 (1963); and A. K. Kerman, L. S. Rodberg, and J. E. Young, Phys. Rev. Letters **11**, 422 (1963).

[30] R. B. Leachman, G. Dearnaley, W. R. Gibbs, and G. G. Seaman, Bull. Am. Phys. Soc. **10**, 463 (1965).

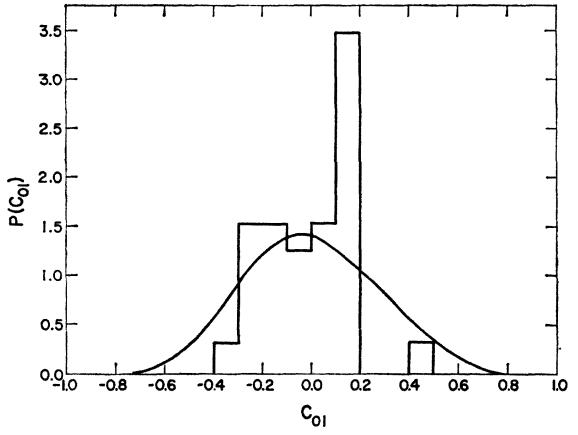

FIG. 16. The frequency distribution function $P(C_{01})$ of the cross correlations C_{01} between data for the same energies ($\epsilon=0$) from the ground- and first-excited-state reactions. The histogram is of data from the 7.25- to 8.11-MeV region. The cross correlations were calculated from Eq. (18). The solid curve was obtained from Monte Carlo calculations with $n=15$ independent points.

averaged compound-nucleus portion of the cross section is obtained. These determinations of direct-interaction and compound-nucleus cross sections were made for the energy range 7.25 to 8.11 MeV, and the results are respectively shown in the upper and lower parts of Fig. 14.

Angular cross-correlation functions were computed in this energy region, and the results of these calculations are shown in Fig. 15. The ground- to first-excited-state cross-correlation functions were also calculated for the various angles, and these results are shown in Fig. 16 along with a curve calculated by the Monte Carlo method[7] for the appropriate sample size.

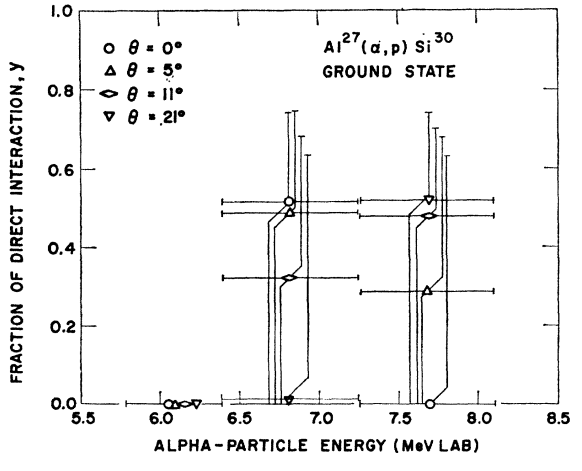

FIG. 17. The fraction y of direct interaction at forward angles as determined from fluctuation analyses. Uncertainties were obtained from the sample sizes n by the method of Ref. 12. The lowest energy points correspond to $R_0(0)$ values so much greater than unity that explanation requires the arguments of Ref. 18.

3. Large Energy Steps for Forward Angles

Since the forward-angle (0°,5°,10°,20°) data were observed over a larger energy range than the intermediate (30°,40°,50°) or back-angle (140°,165°,170°, 175°) data, it is more significant to examine the forward-angle data for the fraction of direct reaction as a function of energy. The results in Fig. 17 are rather uncertain but seem to indicate that only at the highest energies is there any appreciable amount of direct reaction.

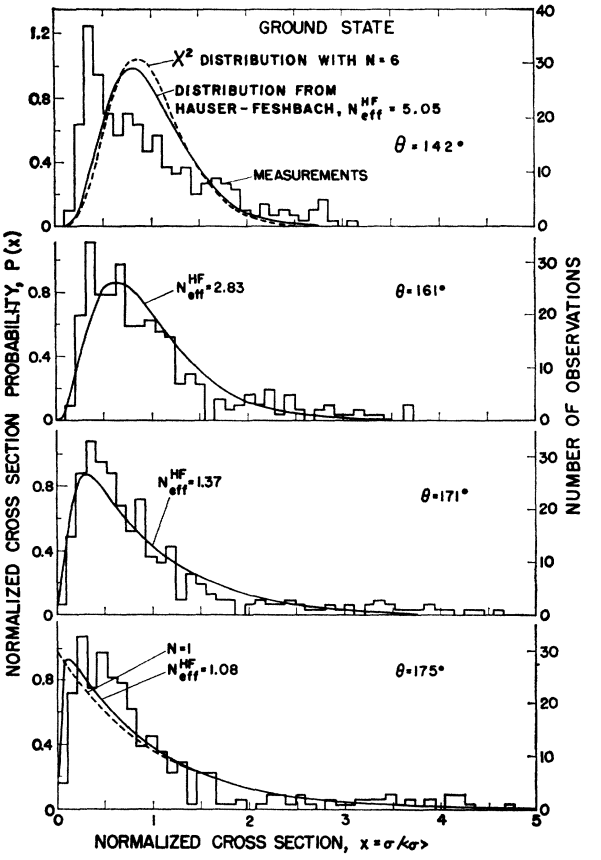

FIG. 18. The frequency functions $P(x)$ of normalized cross section $x=\sigma/\langle\sigma\rangle$ compared with predictions based on a combination of basic cross sections with averages computed by means of Eq. (4).

4. Large Energy Steps for Back Angles

Since these data have been assumed to contain no direct reaction and have been taken over an angular range which comes very close to the beam axis, the experimental frequency distribution functions $P(x)$ may be compared in Fig. 18 with those predicted by a transmission coefficient (Hauser-Feshbach) calculation. It may be noted that the comparison is reasonable except at 142°. This corresponds to the fact that only for 142° is the $N_{\text{eff}}^{\text{exp}}$ obtained in Fig. 13 significantly less than the calculated $N_{\text{eff}}^{\text{HF}}$. This is thought to be

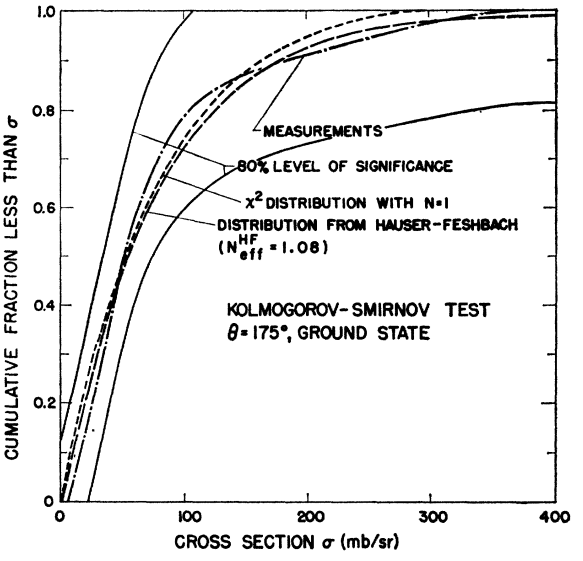

FIG. 19. Kolmogorov-Smirnov test of the Hauser-Feshbach calculated cumulative distribution function and of the approximate case of the simple χ^2 distribution ($N=1$) with the experimental cumulative distribution function. See Sec. IV C 4 for further details.

due to the fact that the number of proton partial waves involved is about four, and the number of independent M states cannot exceed this number. However, all of the M states are assumed to be independent in the Hauser-Feshbach calculation.

Since it is difficult to judge the comparison of frequency distribution functions by eye alone, the Kolmogorov-Smirnov[31] test, which compares cumulative distribution functions, may be used. In Fig. 19 the dot-dash curve is the measured cumulative distribution function for the 175° data. The Kolmogorov-Smirnov test states that, with a 80% level of significance, the actual cumulative distribution function falls between the two solid lines. Thus, the two solid lines act as error indications on the measured cumulative distribution function. The Hauser-Feshbach calculated distribution is seen to fit slightly better than the simple χ^2 (with the lower limit $N=1$, or two degrees of freedom, applicable only for exactly 180°) as expected.

V. DISCUSSION

The purpose of this study is twofold: to investigate the characteristics of fluctuations in the cross sections and to use this technique to extract reaction information.

The most important unresolved problem regarding the first objective was a quantitive treatment of finite sample size effects. By the process of splitting data as described in Sec. IV B, one can make an experimental determination of the behavior of measured quantities as a function of sample size. This experiment has confirmed the theoretical prediction for the expected values of $R(0)$ and Γ for finite sample sizes n, at least for the $Al^{27}(\alpha,p)Si^{30}$ reaction studied. The required corrections due to finite sample size should be particularly useful when small samples are taken to get a quick estimate of the amount of direct reaction or of the coherence width; of course, the corrections are also useful for increasing the reliability of the final results.

In Sec. IV B a method was presented for eliminating nonstationary effects. It is possible to extract the fraction of direct reactions with this method, but this has not yet been attempted. This cannot be done by dividing by a calculated moving average of cross section.

The more conventional analyses[1–3,24] of fluctuation data (e.g., angular cross correlations and state-to-state cross correlation) show good agreement with present data, as was expected. However, it must be noted that the more general form of calculated frequency distribution functions[12] must be used if comparison with data at an arbitrary angle is desired. Another point to remember is that the number of independent M substates is limited by the number of partial waves involved. For this reason one cannot expect low-energy data to assume the large values of N that may be predicted by the spin-degeneracy formula for angles far from the beam axis.

The first information usually obtained about the nucleus itself is the average level width Γ. This was found to behave in agreement with a simple statistical model calculation. This result also fits well the systematics established from light nuclei.[4–7,13–16]

The separation of direct-interaction and compound-nucleus reaction mechanisms is perhaps the most interesting result of the present analysis. Figure 14 has several interesting features. The first thing to be noticed is that the direct-interaction cross section shows the $l=2$ behavior to be expected from the conservation of angular momentum and parity. The second thing to be seen is that the resulting compound-nucleus cross section for the forward angles agrees with the back-angle data. Both show dips at about 40° from the beam axis. In contrast, a Hauser-Feshbach calculation (without corrections for direct reaction) gives an isotropic distribution in this region (within a few percent). This perhaps indicates that an appreciable amount of the total reaction cross section goes by a direct process and that a correction for this is needed.

The present analysis for the fraction y of ground-state direct interaction from Eq. (13) involves $y=0$ for $140°\leq\theta\leq180°$, which is an assumption based on the 175° determination of $y=0$ that results from the use of $N_{\text{eff}}=1$. ($N_{\text{eff}}=1$ is strictly true for 180°, but Figs. 13 and 18 show the calculated $N_{\text{eff}}{}^{\text{HF}}=1.08$ to be sufficiently close to unity.) Under some conditions, the fraction y of direct interactions can be determined

[31] M. G. Kendall and A. Stuart, *The Advanced Theory of Statistics* (Hafner Publishing Company, New York, 1961), Vol. 2, p. 452.

by the method of compound-nucleus fore-aft symmetry

$$(1-y_\theta^2)R^{\pi-\theta}(0)=(1-y_{\pi-\theta}^2)R^\theta(0) \quad (23)$$

and

$$(1-y_\theta)\bar{\sigma}(\theta)=(1-y_{\pi-\theta})\bar{\sigma}(\pi-\theta) \quad (24)$$

even though $N_{\text{eff}}>1$ and both N_{eff} and y initially are unknowns. Superscripts on $R(0)$ and subscripts on y denote the angle. These relations respectively result from the requirement of symmetry about 90° for $N_{\text{eff}}^{\text{exp}}$ [through the use of Eq. (13)] and for $\bar{\sigma}^{\text{CN}}(\theta)$. However, Eqs. (23) and (24) are not independent if $y_\theta=y_{\pi-\theta}$. Thus the fraction y of direct interaction can be obtained from the data through the use of Eqs. (23) and (24) only when $\bar{\sigma}(\theta)$ is significantly different from $\bar{\sigma}(\pi-\theta)$ or, equivalently, when $R^\theta(0)$ is significantly different from $R^{\pi-\theta}(0)$.

We now consider both the ground-state (0^+) and the first-excited-state (2^+) data by the fore-aft symmetry method of Eqs. (23) and (24). For the back angles 140°, 160°, and 170°, the analyses of ground-state data in this paper have been based on an assumed $y_{\pi-\theta}=0$. The forward- and intermediate-angle values of y_θ in the upper part of Fig. 14 that result from Eq. (23) are generally significantly greater than zero. Thus the requirement that Eqs. (23) and (24) be independent is satisfied. The values for $\bar{\sigma}^{\text{CN}}(\theta)$ and $\bar{\sigma}^{\text{CN}}(\pi-\theta)$ obtained from these y_θ and $y_{\pi-\theta}$ values are seen in the lower part of Fig. 14 to conform to the fore-aft symmetry requirement of Eq. (24) by being equal within uncertainties. This then verifies the initial assumption of $y_{\pi-\theta}=0$ at back angles. [Note that $\bar{\sigma}^{\text{CN}}(\pi-\theta)=\bar{\sigma}(\pi-\theta)$ for $y_{\pi-\theta}=0$.]

For the first-excited-state data, any initial determination of the $y_{\pi-\theta}$ value for 175° is complicated by N_{eff} being considerably greater than unity. Furthermore, determinations of the fraction y of direct interactions by Eqs. (23) and (24) are hampered by the fact that the experimental estimates of neither $R_1^\theta(0)$ and $R_1^{\pi-\theta}(0)$ nor $\bar{\sigma}(\theta)$ and $\bar{\sigma}(\pi-\theta)$ generally differ by more than their uncertainties. This is seen by Table II. Thus the $Al^{27}(\alpha,p)Si^{30}$ reaction at our energies has two factors that make determinations of N_{eff} and y difficult: (1) The M substates are not independent, and so calculated estimates of N_{eff} for use in Eq. (13) cannot readily be made and (2) within uncertainties the two equations (23) and (24) are not independent and so cannot provide significant results by this alternative method of compound-nucleus fore-aft symmetry.

TABLE II. Measured average cross sections $\langle\sigma(\theta)\rangle$ and correlation functions $R_1^\theta(0)$ for protons to the first excited state. For 5°, 10°, and 20° data are between $E_\alpha=6.98$ and 8.00 MeV, for 40° between $E_\alpha=7.25$ and 8.00 MeV, and for 140°, 160°, 170°, and 175° between $E_\alpha=7.10$ and 8.00 MeV. Uncertainties are obtained from Ref. 11.

θ	$R_1^\theta(0)$	$R_1^{\pi-\theta}(0)$	$\langle\sigma(\theta)\rangle$ (mb/sr)	$\langle\sigma(\pi-\theta)\rangle$ (mb/sr)
5°	0.29±0.10	0.24±0.10	2.5±0.5	1.8±0.4
10°	0.27±0.10	0.27±0.10	2.4±0.4	1.9±0.4
20°	0.19±0.05	0.18±0.07	2.2±0.4	1.7±0.4
40°	0.12±0.05	0.06±0.03	2.1±0.4	1.0±0.2

Another interesting point concerns the ability of fluctuation analysis to pick intermediate structure[29,30] out of an excitation function. The use of a cross-correlation function seems to hold little promise because of the large uncertainties involved due to finite sample size. If the sample size is increased, the intermediate structure becomes hidden among the statistical fluctuations. One possibility is to work in a region where the separate intermediate structure states are overlapping (as is presumably true in the present case) and hope to find a resonance whose basic behavior is different from those that surround it. Such a basic difference in behavior might be an extreme in the ratio of widths for decay from the simple state into the states of higher complexity (compound-nucleus states in the extreme) and to the free, continuum state. If most of the intermediate structure states decay into the more complex states with an occasional one decaying mostly to the continuum, then this occasional state should appear as a flat region in the cross section. Such a phenomenon is indicated in the present experiment in the first excited state between 8.0- and 8.3-MeV bombarding energy (see Fig. 12). The autocorrelation analyses show this behavior to be outside of statistics, but not sufficiently far for a definite statement to be made.

ACKNOWLEDGMENTS

The authors appreciate the fine self-supporting targets developed by Judith C. Gursky, discussions with R. K. Zeigler on statistical problems, and the bombardments provided by the staff of the Van de Graaff.

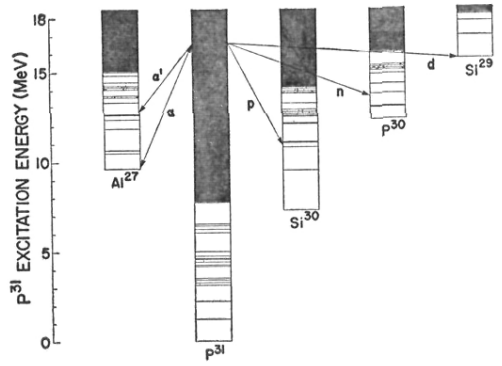

FIG. 1. Exit channels possible for the compound system P^{31}. The figure illustrates a typical excitation energy involved in the experiment. The level positions of some low-lying states of the nuclei are illustrated.